Electrically modulated anomalous phase shift in Andreev bound states mediated by chiral Majorana modes

Yong Xu,[1,2,3] Pei-Hao Fu,[3] Lei Chen,[4] Jun-Feng Liu,[2,*] Jun Wang,[5,†] and Hu Xu[3,‡]

[1]Department of Physics, Harbin Institute of Technology, Harbin 150001, China
[2]School of Physics and Materials Science, Guangzhou University, Guangzhou 510006, China
[3]Department of Physics, Southern University of Science and Technology, Shenzhen 518055, China
[4]College of Science, Beijing University of Civil Engineering and Architecture, Beijing 100044, China
[5]Department of Physics, Southeast University, Nanjing 210096, China

(Received 22 October 2021; revised 14 January 2022; accepted 31 January 2022; published 8 February 2022)

Chiral Majorana modes (CMMs) have attracted considerable interest due to non-Abelian statistics and potential applications in topological quantum computations, but still lack conclusive experimental evidence. Here, we propose that the nonlocal nature of CMMs leads to another transport signature, an anomalous Josephson effect with a tunable ground-state phase difference modulated by a transverse electric field. The CMMs can mediate nonlocal Andreev reflections from the top edge state to the bottom edge state in the quantum anomalous Hall insulator and vice versa. This nonlocal Andreev reflection leads to the spatial separation of electrons and holes. We refer to such Andreev bound states (ABSs) as nonlocal ABSs. It is shown that such nonlocal ABSs and the corresponding Josephson current can be shifted in the dependence on the superconducting phase difference by a transverse electric field. As a result, an electrically modulated anomalous Josephson effect should be observable in experiments. Moreover, when the Josephson junction is sandwiched between two quantum anomalous Hall insulator leads, the electrically tunable phase shift in ABSs results in a conductance oscillation which is applicable in transistors. These findings provide different proposals to experimentally verify the existence of CMMs, and as well as promise potential applications in phase-controllable Josephson devices and topological transistors.

DOI: 10.1103/PhysRevB.105.075409

I. INTRODUCTION

Majorana zero modes in condensed matter systems have attracted considerable interest due to non-Abelian statistics and potential applications in topological quantum computations [1–10]. The one-dimensional chiral Majorana mode (CMM) is predicted to exist on the edge of two-dimensional topological superconductors (TSCs) [11–13] which have been proposed in several systems [14–18]. The most intuitive form of TSCs is the interplay between superconductivity and topological materials [15,19–32]. The quantum anomalous Hall insulator (QAHI) in proximity to an s-wave superconductor has been predicted to be a TSC [19]. The QAHI with Chern number $C = 1$ is topologically equivalent to a chiral topological superconductor (CTSC) with Chern number $N = 2$ when the chemical potential lies in the edge states. By tuning the chemical potential into the bulk states, an $N = 1$ CTSC phase with a single CMM emerges [33]. This system can display novel transport phenomena such as a half-quantized longitudinal conductance plateau [33], perfect crossed Andreev reflection [34], and coherent Majorana transport [35]. However, in the aspect of experimental testing, the important observation of a half-quantized conductance plateau is still under debate regarding the origin of the conductance plateau [36–40].

On the other hand, the anomalous Josephson junction [41–44], namely, the so-called φ_0 junction with an unconventional current-phase relation (CPR) $I(\varphi) = I_c \sin(\varphi - \varphi_0)$, has important applications in superconducting computer memory components [45], superconducting phase batteries and rectifiers [46], as well as flux- or phase-based quantum bits [47]. An anomalous Josephson junction can be realized via the coexistence of spin-orbit coupling and Zeeman field [42,48–51], noncoplanar ferromagnets [52–56], unconventional superconductors [57–61], and the manipulation of topological edge or surface states [62–75]. To our knowledge, an anomalous Josephson junction via CMMs has not been discussed.

A recent work proposed a nonlocal conductance as a fingerprint of CMMs due to the CMM-mediated nonlocal Andreev reflection [76]. The nonlocal Andreev reflection can form nonlocal Andreev bound states (ABSs) in a $N = 1$ TSC/QAHI/$N = 1$ TSC junction. The nonlocal ABSs carry a considerable nonlocal Josephson current which is unique to the $N = 1$ TSC phase with a single CMM [77]. while for the $N = 0$ or $N = 2$ TSC phase, the Josephson current vanishes for a junction with moderate width. This nonlocality in Andreev reflection, ABSs, and Josephson current reveal the

*phjfliu@gzhu.edu.cn
†jwang@seu.edu.cn
‡xuh@sustech.edu.cn

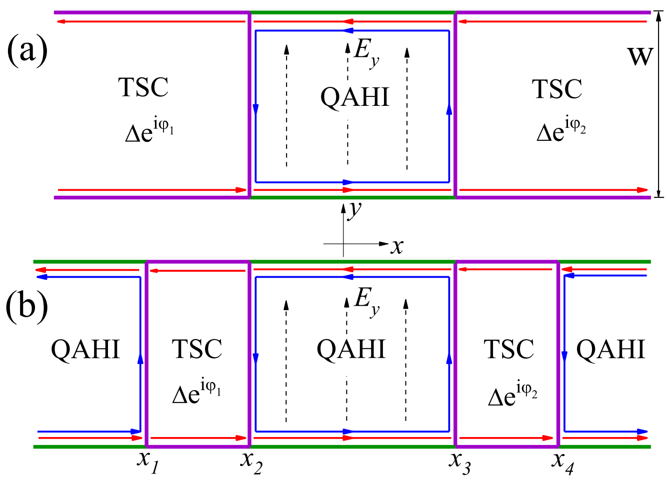

FIG. 1. (a) Schematic diagram of the Josephson junction composed of a QAHI ribbon sandwiched between two $N = 1$ TSC leads. (b) The Josephson junction is sandwiched between two QAHI leads and forms a MJI. The phase difference between two TSCs is $\varphi = \varphi_1 - \varphi_2$ with $\varphi_{1,2}$ the superconducting phase in the left and right TSCs. Chiral Majorana edge modes are depicted along the edges and interfaces. Nonlocal ABSs emerge in the central QAHI region. A transverse electric field E_y is applied in this region to induce an anomalous phase shift in ABSs.

chiral nature of Majorana edge modes, and deserves further exploration.

In this paper, we theoretically show that the nonlocal Josephson current and nonlocal ABSs can be shifted in phase by a transverse electric field due to the spatial separation of the electron and hole. Considering the Josephson junction composed of a QAHI ribbon sandwiched between two $N = 1$ TSCs as shown in Fig. 1(a), right-going electrons (holes) at the bottom edge in the central QAHI will be reflected to left-going holes (electrons) at the top edge with the probability of $1/4$ at the interface between the QAHI and the right TSC. The left-going holes (electrons) are then reflected to right-going electrons (holes) at the bottom edge by the left interface and form a complete ABS. This ABS is nonlocal in that electrons and holes are separated in space by the insulating bulk [78–80]. As a result, a transverse electric field E_y can endow two paired electrons with different potential energies. The difference in the potential will result in different wave vectors of electrons and holes, and then lead to a dynamical phase shift in ABSs due to the traveling of electrons and holes in the central QAHI with finite length. Therefore, an electrically modulated anomalous Josephson effect with an arbitrary ground-state phase difference should be observable in experiments. The manipulation of nonlocal ABSs presents another mechanism to realize the anomalous Josephson effect. Moreover, in a Majorana-Josephson interferometer (MJI) where the Josephson junction is sandwiched between two QAHI leads [35] as shown in Fig. 1(b), the phase shift in ABSs results in a conductance oscillation as the function of E_y in the absence of an external magnetic field. These findings provide different proposals to experimentally identify the existence of CMMs, and as well as promise potential applications in phase-controllable Josephson devices and topological transistors.

The rest of this paper is organized as follows. In Sec. II, we introduce the model of the TSC-QAHI-TSC junction and the MJI, and present the method to calculate the Josephson effect of the Josephson junction and the conductance of the MJI. In Sec. III, we present the numerical results and a discussion on the anomalous Josephson effect. In Sec. IV, the numerical results and a discussion on the conductance oscillation are presented. Finally, a brief summary is given in Sec. V.

II. MODEL AND FORMALISM

The QAHI is described by the low-energy effective Hamiltonian [81,82]

$$H_{\mathrm{QAHI}} = (m - Bk^2)\sigma_z + A(k_x\sigma_x + k_y\sigma_y), \tag{1}$$

where the basis is $(c_{k\uparrow}, c_{k\downarrow})^T$ with $c_{k\uparrow(\downarrow)}$ annihilating an electron with momentum k and spin $\uparrow (\downarrow)$, $\sigma_{x,y,z}$ are the Pauli matrices for spin, A is the strength of spin-orbit coupling, and B and M are material parameters. The QAHI phase emerges for $m/B > 0$. When the QAHI is in proximity to an s-wave superconductor, a nonzero pairing potential Δ can be induced in this system. The Bogoliubov–de Gennes (BdG) Hamiltonian is

$$H_{\mathrm{BdG}} = \begin{pmatrix} H_{\mathrm{QAHI}}(k) - \mu_S & i\Delta\sigma_y \\ -i\Delta^*\sigma_y & -H^*_{\mathrm{QAHI}}(-k) + \mu_S \end{pmatrix}, \tag{2}$$

where the basis is $(c_{k\uparrow}, c_{k\downarrow}, c^\dagger_{-k\uparrow}, c^\dagger_{-k\downarrow})^T$ and μ_S is the chemical potential. When the condition $m^2 < \sqrt{\Delta^2 + \mu_S^2}$ is satisfied, the TSC phase with Chern number $N = 1$ is realized [19,33].

To consider a ribbon geometry in the y direction, we discretize the Hamiltonian in real space along the x and y directions. Then the discretized BdG Hamiltonian is

$$\begin{aligned} H = &\sum_{\mathbf{r}} \Phi^\dagger_{\mathbf{r}} \begin{pmatrix} h(k) - \mu & i\Delta\sigma_y \\ -i\Delta^*\sigma_y & -h^*(-k) + \mu \end{pmatrix} \Phi_{\mathbf{r}} \\ &+ \sum_{\mathbf{r},\mathbf{r}_0} \left[\Phi^\dagger_{\mathbf{r}} \begin{pmatrix} h_{\mathbf{r}_0} & 0 \\ 0 & -h^*_{\mathbf{r}_0} \end{pmatrix} \Phi_{\mathbf{r}+\mathbf{r}_0} + \mathrm{H.c.} \right], \end{aligned} \tag{3}$$

where $\mathbf{r} = (x, y)$ is the site index, $\mathbf{r}_0 = \mathbf{x}$ or $\mathbf{y}$ represents the unit vector along the x or y direction, and $\Phi_{\mathbf{r}} = (c_{\mathbf{r}\uparrow}, c_{\mathbf{r}\downarrow}, c^\dagger_{\mathbf{r}\uparrow}, c^\dagger_{\mathbf{r}\downarrow})^T$ is the field operator with $c_{\mathbf{r}\uparrow(\downarrow)}$ the annihilation operator of an electron at site $\mathbf{r}$ with spin $\uparrow (\downarrow)$. The components included in the Hamiltonian are

$$\begin{aligned} h(k) &= (m - 4B\hbar^2/a^2)\sigma_z, \\ h_{\mathbf{x}} &= (B\hbar^2/a^2)\sigma_z - \frac{i}{2}A\sigma_x, \\ h_{\mathbf{y}} &= (B\hbar^2/a^2)\sigma_z - \frac{i}{2}A\sigma_y, \end{aligned} \tag{4}$$

where a is the lattice constant and $\hbar$ is Planck's constant. The chemical potential $\mu = \mu_N$ in the QAHI region and $\mu = \mu_S$ in the two TSC regions. The superconducting pairing potential $\Delta = 0$ in the QAHI region and $\Delta = \Delta e^{i\varphi_{1,2}}$ with the superconducting phase $\varphi_{1,2}$ in the left and right TSC regions. Moreover, a transverse electric field E_y has also been considered in the normal QAHI region and modeled by linearly increasing on-site energies along the y direction. It can be equivalently modeled by the modification of the chemical potential $\mu_N \rightarrow \mu_N - eE_y y$ with e the unit charge.

By using nonequilibrium Green's functions, the Josephson current through column l in the central QAHI region is calculated by

$$I = \frac{1}{h}\int_{-\infty}^{\infty} \mathrm{Tr}[\check{t}^{\dagger}\check{e}G^{<}_{l,l-1} - \check{e}\check{t}G^{<}_{l-1,l}]dE, \tag{5}$$

where $\check{t} = (B\hbar^2/a^2)\tau_z \otimes \sigma_z + \frac{i}{2}A\tau_0 \otimes \sigma_x$ and $\check{e} = -e\tau_z \otimes \sigma_0$ denote the hopping matrix and the charge matrix, respectively. τ_z (τ_0) is the Pauli (unit) matrix in Nambu space. In equilibrium, the lesser-than Green's function is calculated by $G^< = f(E)[G^a - G^r]$, where $f(E)$ is the Fermi-Dirac distribution function. The retarded and advanced Green's functions read

$$G^r(E) = [G^a(E)]^{\dagger} = \frac{1}{E - H_N - \Sigma^r_L(E) - \Sigma^r_R(E)}, \tag{6}$$

where H_N is the Hamiltonian of the QAHI region. The retarded self-energy $\Sigma^r_{L,R}(E) = [\Sigma^a_{L,R}(E)]^{\dagger}$ due to coupling with the superconducting leads $L(R)$ can be calculated numerically by the recursive method [83,84].

In addition, the ABS spectra can also be numerically calculated through the Green's function technique. The ABSs result in peaks of particle density within the superconducting gap. By searching the peaks of particle density in column l ($x_3 \geqslant l \geqslant x_2$),

$$\rho_l = -\frac{1}{\pi}\mathrm{Im}\{\mathrm{Tr}[G^r(l,l)]\}, \tag{7}$$

at a given phase difference $\varphi = \varphi_L - \varphi_R$, the energies of ABS levels can be located. The ABS spectra are important for understanding the phase shift and the anomalous Josephson current.

For the MJI junction, the conductance can be calculated by means of the lattice Green's function method in the Landauer-Buttiker formalism as [85,86]

$$G = \frac{e^2}{2h}(1 - R + R_A + T - T_A). \tag{8}$$

The normal reflection coefficient R, the normal transmission coefficient T, the local Andreev reflection coefficient R_A, and the crossed Andreev reflection coefficient T_A can be given by [34]

$$\begin{aligned} T &= \mathrm{Tr}\left(\Gamma^L_{ee}G^r_{ee}\Gamma^R_{ee}G^a_{ee}\right),\\ R_A &= \mathrm{Tr}\left(\Gamma^L_{ee}G^r_{eh}\Gamma^L_{hh}G^a_{he}\right),\\ T_A &= \mathrm{Tr}\left(\Gamma^L_{ee}G^r_{eh}\Gamma^R_{hh}G^a_{he}\right),\\ R &= \mathrm{Tr}\left(\Gamma^L_{ee}G^r_{ee}\Gamma^L_{ee}G^a_{ee}\right) + iTr\left[\Gamma^L_{ee}\left(G^a_{ee} - G^r_{ee}\right)\right] + 1, \end{aligned} \tag{9}$$

where e (h) represent electron (hole), and $\Gamma^{L,R} = i[\Sigma^r_{L,R} - \Sigma^a_{L,R}]$ are the linewidth functions of left and right leads coupled to the central scattering region.

III. ANOMALOUS JOSEPHSON EFFECT

In this section, we present the numerical results and discussions on the electrically modulated anomalous Josephson effect in the TSC-QAHI-TSC junction as shown in Fig. 1(a). We consider a right-going electron in the central QAHI region which is localized at the bottom edge and can be viewed as the superposition of two CMMs [19,33]. At first, the electron travels from the left interface to the right interface and accumulates a dynamic phase $k_{e+}L$, where k_{e+} is the wave vector of right-going electron edge mode and L is the length of QAHI region. Then, mediated by the single CMM at the QAHI-TSC interface, the electron will be reflected as either an electron or a hole at the top edge, with the same probability of $1/4$ [33,76]. The hole will travel from the right interface to the left interface and accumulates a dynamic phase $k_{h-}L$, where k_{h-} is the wave vector of the left-going hole edge mode. Then, the hole will be reflected as an electron with the probability of $1/4$, which finishes a cycle to form an Andreev bound state. It is clearly seen that this ABS is chiral and nonlocal, and travels around along the edges of QAHI region. Note that the nonlocality of the ABS is attributed to the CMMs traveling along the two interfaces. Without the CMMs, the coupling between electrons and holes which are separated by the insulating bulk, can be induced only by the superposition of edge states, i.e., the finite-size effect, and will vanish when the width of the ribbon increases [77]. Therefore, a nonlocal ABS with spatially separated electrons and holes is the unique signature of Josephson junctions with CMMs.

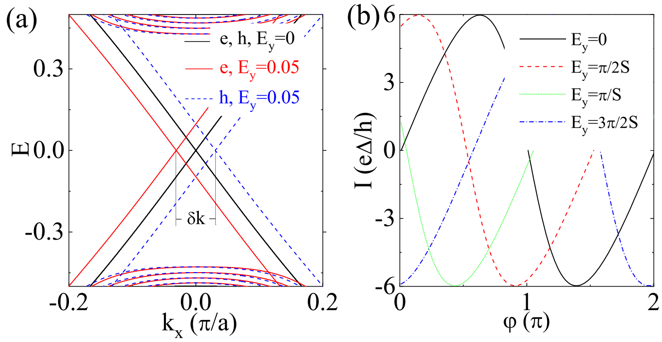

FIG. 2. (a) Spectra of electrons and holes in the QAHI ribbon in the absence of transverse electric field (black solid lines). In the presence of a transverse field, the electron energy bands move in the $-k_x$ direction (red solid lines) and the hole energy bands move in the k_x direction (blue dashed lines). The transverse field is $E_y = 0.003$. (b) Current phase relationship for different anomalous phases of the transverse field E_y which varies from 0 to $3\pi/2S$ with the junction area $S = W * L$. The temperature $T = 0.001T_c$, where T_c is the critical temperature. The dimensions of the QAHI region are $W = 100a$ and $L = 100a$, and the other parameters are $A = B = 1$, $m = -0.5$, $\mu_N = 0$, $\mu_s = 1$, $\Delta = 0.35$.

Due to the spatial separation of electrons and holes in the ABSs, a transverse electrical field will cause an important consequence. The transverse electric field E_y can be modeled by a linearly distributed on-site potential. Therefore, the separation of electrons and holes in space makes it possible that E_y endows two paired electrons with different potential energies. For $\mu_N = 0$, the spectra of electrons and holes in the QAHI are shown in Fig. 2(a). When $E_y = 0$, the spectra of electrons and holes superpose. With finite E_y, the energy of the right-going electron at the bottom edge increase while that of the left-going electron at the top edge decrease. Equivalently, it is seen that the spectra of electrons move left towards the

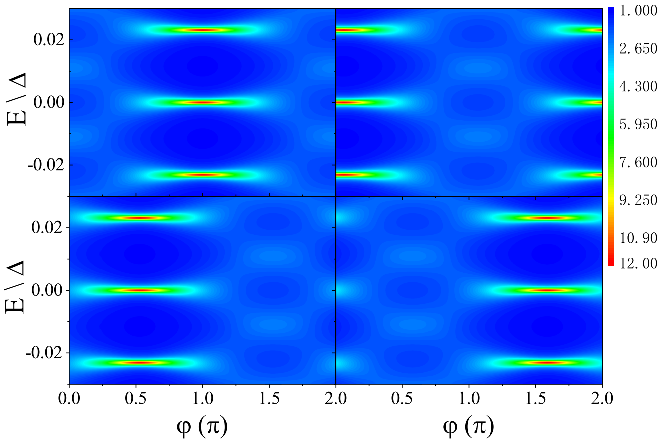

FIG. 3. ABS spectra with various transverse electric fields (a) $E_y = 0$, (b) $E_y = \pi/2S$, (c) $E_y = \pi/S$, and (d) $E_y = 3\pi/2S$. Other parameters are the same as those in Fig. 2(b).

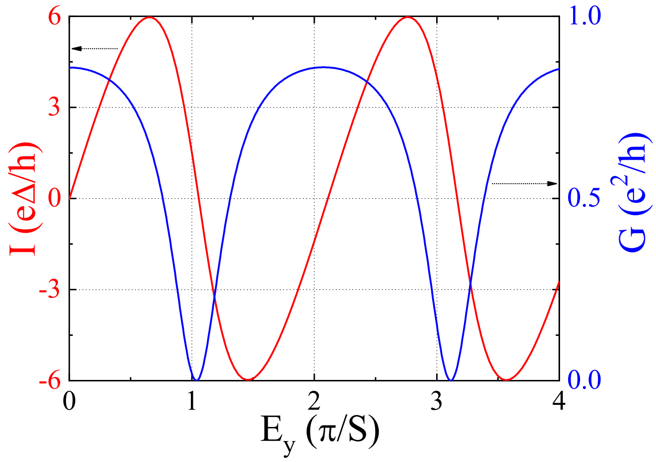

FIG. 4. The relationship of the Josephson current (red) and the transverse field and the relationship of the conductance (red) and the transverse field with superconductor phase difference $\varphi = 0$. The length of TSC is $x_2 - x_1 = x_4 - x_3 = 60a$ and the width is $W = 100a$. Other parameters are the same as those in Fig. 2(b).

$-k_x$ direction. On the contrary, the spectra of holes move right towards the positive direction.

The wave vector difference δk between electrons and holes will lead to an extra phase δkL in the formation of ABS due to the traveling of electrons and holes in the QAHI region. The wave vector difference δk can be estimated by $\delta k = k_x^e - k_x^h = -E_y W/A$ with W the width of the QAHI ribbon. Therefore, the anomalous phase shift is $\varphi_0 = \delta kL = -E_y S/A$ with $S = W * L$ the area of the QAHI region. Then the Josephson current will correspondingly have an anomalous phase shift, $I = I_c \sin(\varphi + \varphi_0)$, where $\varphi = \varphi_1 - \varphi_2$ is the phase difference between the two TSCs with superconducting phase $\varphi_{1,2}$ and I_c is the critical Josephson current. The nonlocal ABSs and linear dependence of the ground-state phase difference φ_0 on the transverse electric field is a signature of CMMs. In the other φ_0 junctions without CMMs, such dependence of φ_0 on the transverse electric field will not be observed.

Figure 2(b) shows the CPR for various values of E_y. In the process of numerical calculation, we take parameters $A = B = 1$, $m = -0.5$, $\mu_N = 0$, $\mu_s = 1$, $\Delta = 0.35$, $W = 100a$, and $L = 100a$. The CPR displays a distorted sinusoid due to the low temperature $T = 0.001T_c$ with T_c the critical temperature. It is clearly seen that the anomalous phase shift φ_0 increases linearly with increasing E_y while the critical current I_c almost remains unchanged, which is consistent with our above estimation. Moreover, the numerical results of ABSs (shown in Fig. 3) also verify the same E_y-induced anomalous phase shift φ_0. It is concluded that the nonlocal Josephson current and nonlocal ABSs can be shifted in phase by a transverse electric field due to the spatial separation of electrons and holes.

IV. CONDUCTANCE OSCILLATION IN MJI

In addition to the anomalous Josephson effect, the anomalous phase shift in ABSs can also induce an oscillation of the two-terminal conductance in the MJI junction (QAHI-TSC-QAHI-TSC-QAHI junction) as shown in Fig. 1(b). In the absence of a transverse electric field, when the phase difference φ between the two TSCs equals π, one set of ABS levels near the zero energy crosses the zero energy exactly. It is shown that the wave functions of CMMs at the top and bottom edges of two TSCs are orthogonal to each other, i.e., $\langle\Psi_{\mathrm{TSC1}}|\Psi_{\mathrm{TSC2}}\rangle = \cos(\varphi/2) = 0$ [35]. Hence, the conductance of the MJI junction vanishes and reaches a minimum with varying phase difference φ. From the above discussion of the anomalous Josephson current, we know that the E_y-induced anomalous phase shift φ_0 is fully equivalent to φ. Therefore, we expect a conductance oscillation tuned by the transverse electric field E_y in the MJI junction without a magnetic field [35].

Figure 4 shows the Josephson current and the MJI conductance as functions of the transverse electric field E_y when the superconducting phase difference $\varphi = 0$. The anomalous Josephson current displays a sinusoidal dependence on E_y, which verifies that φ_0 is fully equivalent to φ. The MJI conductance also displays a periodic oscillation over E_y. Approximately when the E_y-induced anomalous phase shift $\varphi_0 = (2n+1)\pi$, the conductance reaches its minimum which is close to zero. The deviation of the period in E_y away from $2\pi/S$ is attributed to the side effect of E_y and grows with increasing E_y. For a large area S, only a weak electric field E_y is necessary and then the side effect can be suppressed. To verify this argument, we also plot the conductance oscillation as the function of the length $L = x_3 - x_2$ of the QAHI region when a small $E_y = 0.02\pi$ is applied, as shown in Fig. 5. The perfect oscillation over the length shows that the period in L is very close to $100a$ and the side effect of E_y is well suppressed. This conductance oscillation is also the unique signature of CMMs and will not appear in other Josephson interferometers. For potential applications, the conductance oscillation can be applicable in CMM-based topological transistors.

V. CONCLUSION

In summary, we propose to employ a transverse electric field to introduce a phase shift in the nonlocal CMM-mediated ABSs in a QAHI sandwiched between two $N = 1$ TSCs.

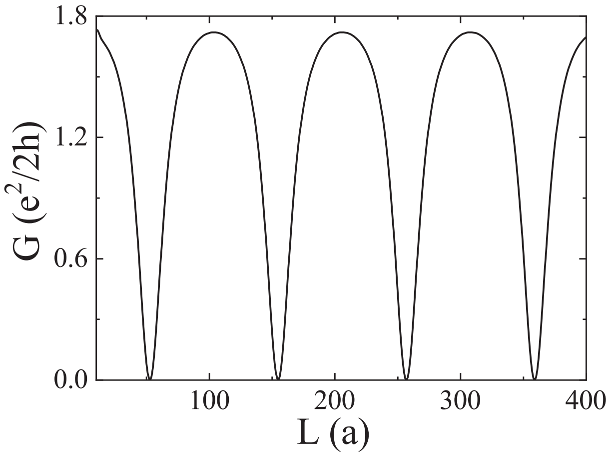

FIG. 5. The relationship of the conductance and length of QAHI region with superconductor phase difference $\varphi = 0$ and the transverse field $E_y = 0.02\pi$. Other parameters are the same as those in Fig. 4.

This phase shift results in an anomalous Josephson effect in TSC-QAHI-TSC junctions where the ground-state phase difference becomes arbitrary, other than 0 or π, and tunable by a transverse electric field. Furthermore, in the QAHI-TSC-QAHI-TSC-QAHI junction which is also referred to as the MJI junction, the anomalous phase shift in the nonlocal ABSs is shown to lead to a conductance oscillation as the function of the transverse electric field. Compared with previous φ_0 junctions, the nonlocal ABSs, linear dependence of φ_0 on the transverse electric field, and the conductance oscillation in the MJI junction are unique signatures of CMMs. These results provide complementary experimental proposals to identify the existence of CMMs and promise potential applications in phase-controllable Josephson devices and CMM-based topological transistors.

ACKNOWLEDGMENTS

The work described in this paper is supported by National Natural Science Foundation of China (NSFC, Grants No. 12174077 and No. 12174051), and National Natural Science Foundation of Guangdong Province (Grant No. 2021A1515012363). L.C. is thankful for support by the general Program of Science and Technology Development Project of Beijing Municipal Education Commission No. KM201910016002.

[1] A. Y. Kitaev, Phys.-Usp. **44**, 131 (2001).
[2] F. Wilczek, Nat. Phys. **5**, 614 (2009).
[3] C. Nayak, S. H. Simon, A. Stern, M. Freedman, and S. Das Sarma, Rev. Mod. Phys. **80**, 1083 (2008).
[4] J. Alicea, Rep. Prog. Phys. **75**, 076501 (2012).
[5] H. Zhang, D. E. Liu, M. Wimmer, and L. P. Kouwenhoven, Nat. Commun. **10**, 5128 (2019).
[6] S. D. Sarma, M. Freedman, and C. Nayak, npj Quantum Inf. **1**, 15001 (2015).
[7] D. Litinski, M. S. Kesselring, J. Eisert, and F. von Oppen, Phys. Rev. X **7**, 031048 (2017).
[8] R. M. Lutchyn, E. P. A. M. Bakkers, L. P. Kouwenhoven, P. Krogstrup, C. M. Marcus, and Y. Oreg, Nat. Rev. Mater. **3**, 52 (2018).
[9] C. Schrade and L. Fu, Phys. Rev. Lett. **120**, 267002 (2018).
[10] J. Sau and S. Tewari, arXiv:2105.03769.
[11] X.-L. Qi and S.-C. Zhang, Rev. Mod. Phys. **83**, 1057 (2011).
[12] C. Beenakker, Annu. Rev. Condens. Matter Phys. **4**, 113 (2013).
[13] M. Sato and Y. Ando, Rep. Prog. Phys. **80**, 076501 (2017).
[14] A. Kitaev, Ann. Phys. **321**, 2 (2006).
[15] L. Fu and C. L. Kane, Phys. Rev. Lett. **100**, 096407 (2008).
[16] A. Stern, Nature (London) **464**, 187 (2010).
[17] J. D. Sau, R. M. Lutchyn, S. Tewari, and S. Das Sarma, Phys. Rev. Lett. **104**, 040502 (2010).
[18] J. Alicea, Phys. Rev. B **81**, 125318 (2010).
[19] X.-L. Qi, T. L. Hughes, and S.-C. Zhang, Phys. Rev. B **82**, 184516 (2010).
[20] T. Meng and L. Balents, Phys. Rev. B **86**, 054504 (2012).
[21] G. Bednik, A. A. Zyuzin, and A. A. Burkov, Phys. Rev. B **92**, 035153 (2015).
[22] S. Kobayashi and M. Sato, Phys. Rev. Lett. **115**, 187001 (2015).
[23] R. Nandkishore, Phys. Rev. B **93**, 020506(R) (2016).
[24] M. Alidoust, K. Halterman, and A. A. Zyuzin, Phys. Rev. B **95**, 155124 (2017).
[25] Y. Wang and R. M. Nandkishore, Phys. Rev. B **95**, 060506(R) (2017).
[26] A.-Q. Wang, C.-Z. Li, C. Li, Z.-M. Liao, A. Brinkman, and D.-P. Yu, Phys. Rev. Lett. **121**, 237701 (2018).
[27] C. Huang, B. T. Zhou, H. Zhang, B. Yang, R. Liu, H. Wang, Y. Wan, K. Huang, Z. Liao, E. Zhang, S. Liu, Q. Deng, Y. Chen, X. Han, J. Zou, X. Lin, Z. Han, Y. Wang, K. T. Law, and F. Xiu, Nat. Commun. **10**, 2217 (2019).
[28] J. J. He, T. Liang, Y. Tanaka, and N. Nagaosa, Commun. Phys. **2**, 149 (2019).
[29] S. M. Frolov, M. J. Manfra, and J. D. Sau, Nat. Phys. **16**, 718 (2020).
[30] P.-H. Fu, J.-F. Liu, and J. Wu, Phys. Rev. B **102**, 075430 (2020).
[31] C.-Z. Li, A.-Q. Wang, C. Li, W.-Z. Zheng, A. Brinkman, D.-P. Yu, and Z.-M. Liao, Phys. Rev. Lett. **126**, 027001 (2021).
[32] Y. Wang, G.-H. Lee, and M. N. Ali, Nat. Phys. **17**, 542 (2021).
[33] S. B. Chung, X.-L. Qi, J. Maciejko, and S.-C. Zhang, Phys. Rev. B **83**, 100512(R) (2011).
[34] Y.-T. Zhang, Z. Hou, X. C. Xie, and Q.-F. Sun, Phys. Rev. B **95**, 245433 (2017).
[35] C.-A. Li, J. Li, and S.-Q. Shen, Phys. Rev. B **99**, 100504(R) (2019).
[36] Q. L. He, L. Pan, A. L. Stern, E. C. Burks, X. Che, G. Yin, J. Wang, B. Lian, Q. Zhou, E. S. Choi *et al.*, Science **357**, 294 (2017).
[37] W. Ji and X.-G. Wen, Phys. Rev. Lett. **120**, 107002 (2018).
[38] Y. Huang, F. Setiawan, and J. D. Sau, Phys. Rev. B **97**, 100501(R) (2018).
[39] J. Shen, J. Lyu, J. Z. Gao, Y.-M. Xie, C.-Z. Chen, C.-w. Cho, O. Atanov, Z. Chen, K. Liu, Y. J. Hu *et al.*, Proc. Natl. Acad. Sci. USA **117**, 238 (2020).

[40] M. Kayyalha, D. Xiao, R. Zhang, J. Shin, J. Jiang, F. Wang, Y.-F. Zhao, R. Xiao, L. Zhang, K. M. Fijalkowski *et al.*, Science **367**, 64 (2020).

[41] A. A. Reynoso, G. Usaj, C. A. Balseiro, D. Feinberg, and M. Avignon, Phys. Rev. Lett. **101**, 107001 (2008).

[42] A. Buzdin, Phys. Rev. Lett. **101**, 107005 (2008).

[43] A. Zazunov, R. Egger, T. Jonckheere, and T. Martin, Phys. Rev. Lett. **103**, 147004 (2009).

[44] J.-F. Liu and K. S. Chan, Phys. Rev. B **82**, 125305 (2010).

[45] E. C. Gingrich, B. M. Niedzielski, J. A. Glick, Y. Wang, D. L. Miller, R. Loloee, W. P. Pratt, Jr., and N. O. Birge, Nat. Phys. **12**, 564 (2016).

[46] A. A. Reynoso, G. Usaj, C. A. Balseiro, D. Feinberg, and M. Avignon, Phys. Rev. B **86**, 214519 (2012).

[47] C. Padurariu and Y. V. Nazarov, Phys. Rev. B **81**, 144519 (2010).

[48] A. G. Mal'shukov, Phys. Rev. B **97**, 064515 (2018).

[49] Y. M. Shukrinov, I. R. Rahmonov, and K. Sengupta, Phys. Rev. B **99**, 224513 (2019).

[50] M. Alidoust, Phys. Rev. B **101**, 155123 (2020).

[51] M. Alidoust, C. Shen, and I. Žutić, Phys. Rev. B **103**, L060503 (2021).

[52] V. Braude and Y. V. Nazarov, Phys. Rev. Lett. **98**, 077003 (2007).

[53] J.-F. Liu and K. S. Chan, Phys. Rev. B **82**, 184533 (2010).

[54] J.-F. Liu, K. Sum Chan, and J. Wang, J. Phys. Soc. Jpn. **80**, 124708 (2011).

[55] M. Alidoust, M. Willatzen, and A.-P. Jauho, Phys. Rev. B **98**, 184505 (2018).

[56] K. Halterman, M. Alidoust, R. Smith, and S. Starr, arXiv:2111.01242.

[57] M. H. S. Amin, A. N. Omelyanchouk, and A. M. Zagoskin, Phys. Rev. B **63**, 212502 (2001).

[58] P. E. C. Ashby and C. Kallin, Phys. Rev. B **79**, 224509 (2009).

[59] J.-F. Liu, J. Phys. Soc. Jpn. **83**, 024712 (2014).

[60] H. Zhang, J. Wang, and J.-F. Liu, Appl. Phys. Lett. **108**, 102601 (2016).

[61] J.-F. Liu, Y. Xu, and J. Wang, Sci. Rep. **7**, 43899 (2017).

[62] Y. Tanaka, T. Yokoyama, and N. Nagaosa, Phys. Rev. Lett. **103**, 107002 (2009).

[63] F. Dolcini, M. Houzet, and J. S. Meyer, Phys. Rev. B **92**, 035428 (2015).

[64] J. Wang, L. Hao, and J.-F. Liu, Phys. Rev. B **93**, 155405 (2016).

[65] A. Zyuzin, M. Alidoust, and D. Loss, Phys. Rev. B **93**, 214502 (2016).

[66] I. V. Bobkova, A. M. Bobkov, A. A. Zyuzin, and M. Alidoust, Phys. Rev. B **94**, 134506 (2016).

[67] X. Zhou and G. Jin, Phys. Rev. B **95**, 195419 (2017).

[68] M. Alidoust and H. Hamzehpour, Phys. Rev. B **96**, 165422 (2017).

[69] M. Alidoust, M. Willatzen, and A.-P. Jauho, Phys. Rev. B **98**, 085414 (2018).

[70] M. Alidoust, Phys. Rev. B **98**, 245418 (2018).

[71] Y. Xu, S. Uddin, J. Wang, Z. Ma, and J.-F. Liu, Phys. Rev. B **97**, 035427 (2018).

[72] P.-H. Fu, J. Wang, J.-F. Liu, and R.-Q. Wang, Phys. Rev. B **100**, 115414 (2019).

[73] M. Alidoust and K. Halterman, Phys. Rev. B **101**, 035120 (2020).

[74] K. Kulikov, D. Sinha, Y. M. Shukrinov, and K. Sengupta, Phys. Rev. B **101**, 075110 (2020).

[75] D. Sinha, Phys. Rev. B **102**, 085144 (2020).

[76] S. Ikegaya, Y. Asano, and D. Manske, Phys. Rev. Lett. **123**, 207002 (2019).

[77] C.-Z. Chen, J. J. He, D.-H. Xu, and K. T. Law, Phys. Rev. B **98**, 165439 (2018).

[78] J. Liu, H. Liu, J. Song, Q.-F. Sun, and X. C. Xie, Phys. Rev. B **96**, 045401 (2017).

[79] J. A. M. van Ostaay, A. R. Akhmerov, and C. W. J. Beenakker, Phys. Rev. B **83**, 195441 (2011).

[80] B. Baxevanis, V. P. Ostroukh, and C. W. J. Beenakker, Phys. Rev. B **91**, 041409(R) (2015).

[81] X.-L. Qi, Y.-S. Wu, and S.-C. Zhang, Phys. Rev. B **74**, 085308 (2006).

[82] C.-X. Liu, S.-C. Zhang, and X.-L. Qi, Annu. Rev. Condens. Matter Phys. **7**, 301 (2016).

[83] D. H. Lee and J. D. Joannopoulos, Phys. Rev. B **23**, 4988 (1981).

[84] D. H. Lee and J. D. Joannopoulos, Phys. Rev. B **23**, 4997 (1981).

[85] *Electronic Transport in Mesoscopic Systems*, edited by S. Datta (Cambridge University Press, Cambridge, UK, 1995).

[86] J. Li, G. Fleury, and M. Büttiker, Phys. Rev. B **85**, 125440 (2012).